Cell, Vol. 110, 737–749, September 20, 2002, Copyright ©2002 by Cell Press

Regulation of Myocardial Contractility and Cell Size by Distinct PI3K-PTEN Signaling Pathways

Michael A. Crackower,[1,2,15,16] Gavin Y. Oudit,[3,16] Ivona Kozieradzki,[1,2] Renu Sarao,[1,2] Hui Sun,[3] Takehiko Sasaki,[4,5] Emilio Hirsch,[6] Akira Suzuki,[7] Tetsuo Shioi,[8] Junko Irie-Sasaki,[4,5] Rajan Sah,[3] Hai-Ying M. Cheng,[1,2] Vitalyi O. Rybin,[9] Giuseppe Lembo,[10] Luigi Fratta,[10] Antonio J. Oliveira-dos-Santos,[2] Jeffery L. Benovic,[11] C. Ronald Kahn,[12] Seigo Izumo,[8] Susan F. Steinberg,[9] Matthias P. Wymann,[13] Peter H. Backx,[3] and Josef M. Penninger[1,2,14]

[1]IMBA
Institute for Molecular Biotechnology of the Austrian Academy of Sciences
c/o Dr. Bohr Gasse 7
A-1030 Vienna
Austria

[2]Ontario Cancer Institute
Departments of Medical Biophysics and Immunology
University of Toronto
620 University Avenue
Toronto, Ontario
Canada M5G 2C1

[3]Departments of Physiology and Medicine and the University Health Network
Richard Lewar/Heart and Stroke Centre of Excellence
University of Toronto
Toronto
Canada

[4]Department of Pharmacology
The Tokyo Metropolitan Institute of Medical Science
Tokyo
Japan

[5]PRESTO
Japan Science and Technology Corporation (JST)
Tokyo
Japan

[6]Dipartimento di Genetica, Biologia, e Biochimica
Universita di Torino
10126 Torino
Italy

[7]Department of Biochemistry
Akita University School of Medicine
Akita 010-8543
Japan

[8]Cardiovascular Division
Beth Israel Deaconess Medical Center
Harvard Medical School
Boston, Massachusetts 02215

[9]Departments of Pharmacology and Medicine
Columbia University
New York, New York 10032

[10]Department of Neurocardiology
Neuromed Institute
Pozzilli (Isernia)
Italy

[11]Departments of Microbiology and Immunology
Kimmel Cancer Center
Thomas Jefferson University
Philadelphia, Pennsylvania 19107

[12]Research Division
Joslin Diabetes Center
Harvard Medical School
Boston, Massachusetts 02215

[13]Department of Medicine
Division of Biochemistry
University of Fribourg
CH-1700 Fribourg
Switzerland

[14]Correspondence: jpenning@uhnres.utoronto.ca
[15]Present address: Amgen Inc., Thousand Oaks, California 91320.
[16]These authors contributed equally to this work.

Summary

The PTEN/PI3K signaling pathway regulates a vast array of fundamental cellular responses. We show that cardiomyocyte-specific inactivation of tumor suppressor PTEN results in hypertrophy, and unexpectedly, a dramatic decrease in cardiac contractility. Analysis of double-mutant mice revealed that the cardiac hypertrophy and the contractility defects could be genetically uncoupled. PI3Kα mediates the alteration in cell size while PI3Kγ acts as a negative regulator of cardiac contractility. Mechanistically, PI3Kγ inhibits cAMP production and hypercontractility can be reverted by blocking cAMP function. These data show that PTEN has an important in vivo role in cardiomyocyte hypertrophy and GPCR signaling and identify a function for the PTEN-PI3Kγ pathway in the modulation of heart muscle contractility.

Introduction

Cardiovascular diseases are predicted to be the most common cause of death worldwide by 2020 (Yusuf et al., 2001). Cardiovascular disease is frequently associated with elevated wall stress as a result of pressure overload, such as in hypertension or volume overload seen in valvular disorders. Increased wall stress in the heart triggers a hypertrophic response (Hunter and Chien, 1999). What is initially a compensatory response, pathological hypertrophy eventually leads to decompensation resulting in left ventricle dilation, myocyte loss, increased interstitial fibrosis, and heart failure. While increased wall stress can lead to pathological cardiac hypertrophy, increased demand for cardiac output can also cause a physiological increase in cell size, as commonly seen in endurance athletes (Colan, 1997).

In flies and mammals, hypertrophic responses can be initiated via phosphoinositide 3-kinase (PI3K) signaling pathways (Leevers et al., 1996; Shioi et al., 2000). PI3Ks constitute a family of evolutionarily conserved lipid ki-

nases that regulate a vast array of fundamental cellular responses, including proliferation, adhesion, cell size, and protection from apoptosis (Toker and Cantley, 1997; Stephens et al., 1993). These responses result from the activation of membrane trafficking proteins and enzymes such as the phosphoinositide-dependent kinases (PDKs), PKB/Akt, or S6 kinases by the key second messenger PIP3 (Franke et al., 1997; Alessi et al., 1998; Downward, 1998). Four different type I PI3Ks have been described three of which (PI3Kα, β, δ) are activated by receptor tyrosine kinase pathways. PI3Kγ is activated by the $\beta\gamma$ subunit of G-proteins and acts downstream of G protein-coupled receptors (GPCRs; Toker and Cantley, 1997). Recent genetic evidence in hematopoietic cells indicates that PI3Kγ is the sole PI3K that couples to GPCRs (Sasaki et al., 2000; Hirsch et al., 2000; Li et al., 2000).

In isolated cardiomyocytes, PI3K signaling has been implicated as a component of cardiac hypertrophy and protection of myocytes from apoptosis mediated by numerous exogenous agonists and stresses (Rabkin et al., 1997; Schluter et al., 1999; Baliga et al., 1999; Kodama et al., 2000). In transgenic mice, overexpression of constitutively active p110α results in increased heart size, whereas cardiac overexpression of dominant-negative p110α in mice resulted in smaller hearts without affecting heart functions (Shioi et al., 2000). Furthermore, PI3Kγ activity is increased upon aortic constriction in mice (Naga Prasad et al., 2000), suggesting that both tyrosine-based and GPCR-linked PI3Ks might play a role in the cardiac hypertrophy response.

The tumor suppressor PTEN is a lipid phosphatase that dephosphorylates the D3 position of PIP3 (Maehama and Dixon, 1998). Thus, PTEN lowers the levels of the PI3K product PIP3 within the cells and antagonizes PI3K mediated cellular signaling. It has been recently shown that PTEN can regulate neuronal stem cell proliferation and the cell size of neurons in brain-specific PTEN mouse mutants similar to patients with Lhermitte-Duclos disease (Backman et al., 2001). Moreover, expression of dominant-negative PTEN in rat cardiomyocytes in tissue culture results in hypertrophy (Schwartzbauer and Robbins, 2001). Whether PI3Ks and PTEN can indeed control cardiac hypertrophy and heart functions in vivo is not known.

We investigated the role of the PI3K-PTEN signaling pathway in cardiac hypertrophy by studying *PTEN*-heart muscle specific mutant mice, *p110*$\gamma^{-/-}$, dominant-negative *p110*α transgenic mice, and double-mutant mice. We show that two independent PI3K signaling pathways exist in cardiomyocytes that can be genetically uncoupled. While the tyrosine kinase-receptor p110α-PTEN pathway is a critical regulator of cardiac cell size, the GPCR-linked PI3Kγ-PTEN signaling pathway modulates heart muscle contractility.

Results

Generation of Cardiac Muscle Specific PTEN Knockout Mice

Inactivation of PTEN in all cells results in early embryonic lethality between day 6.5 to 9.5 (Suzuki et al., 1998; Di Cristofano et al., 1998). We therefore used a tissue specific gene targeting approach to mutate PTEN in all cardiomyocytes and skeletal muscle cells. Mice that have exon 4 and 5 of PTEN flanked by loxP sites by homologous recombination (PTEN^{flox}; Suzuki et al., 2001) were mated with a CRE deleter line that expresses the CRE transgene under the control of the muscle creatinine kinase promoter (mckCRE; Bruning et al., 1998). We generated homozygous mutant mice that express CRE and are floxed at both PTEN alleles (mckCRE-PTEN$^{\Delta/\Delta}$), heterozygous mice that express CRE but are only floxed at one PTEN allele (mckCRE-PTEN$^{\Delta/+}$), and control mice that do not express mckCRE but have both PTEN alleles floxed (PTEN$^{flox/flox}$). No phenotypic differences between mckCRE-PTEN$^{\Delta/+}$ and PTEN$^{flox/flox}$ genotypes were observed. Western blotting showed a significant reduction in the amount of PTEN protein in both the heart as well as skeletal muscle, but no other tissues, of mckCRE-PTEN$^{\Delta/\Delta}$ mice (Figure 1A). The presence of residual PTEN protein in mckCRE-PTEN$^{\Delta/\Delta}$ mice is likely due to PTEN expression in cardiac non-myocyte cell types such as endothelial cells or fibroblasts. Hearts from mckCRE-PTEN$^{\Delta/\Delta}$ mice showed no alteration in the expression of PI3Kα, PI3Kβ, or PI3Kγ catalytic subunits nor changes in p85α expression (Figure 1B).

Spontaneous Cardiac Hypertrophy in PTEN-Deficient Hearts

Analysis of skeletal muscle from mckCRE-PTEN$^{\Delta/\Delta}$ mice showed no gross abnormalities or any overt changes in cell size compared to control mckCRE-PTEN$^{\Delta/+}$ or PTEN$^{flox/flox}$ littermates. Overall body weights were comparable between all three genotypes at all ages analyzed (10 wks, 6 months, and 12 months). Moreover, there was no indication of diabetes and blood glucose levels did not differ between mckCRE-PTEN$^{\Delta/\Delta}$, mckCRE-PTEN$^{\Delta/+}$, and PTEN$^{flox/flox}$ littermates.

Whereas skeletal muscle appeared normal, loss of PTEN in cardiac muscle resulted in greatly increased heart sizes in the mutant mckCRE-PTEN$^{\Delta/\Delta}$ mice (Figures 1C and 1D). Concordantly, there was a significant increase in heart/body weight ratios in the PTEN-deficient hearts indicative of cardiac hypertrophy at 10 weeks and 12 months of age (Figure 2A). The increased heart size was already detectable in newborn mckCRE-PTEN$^{\Delta/\Delta}$ mice (not shown). Histologically, the increase in heart size was observed throughout the heart (Figure 1D). Interestingly, cardiac hypertrophy did not result in fibrotic or structural changes in myocyte organization (Figure 1D) or perturbations in cardiomyocyte cell death (not shown) even at 1 year of age indicating that loss of PTEN does not result in cardiac decompensation or dilated cardiomyopathy.

To further analyze the cardiac hypertrophy in PTEN-deficient hearts, cardiomyocytes were isolated from adult mice to assess the individual cell size. Loss of PTEN resulted in a marked increase in both the length and width of cardiomyocytes as compared to controls (Figure 2B). The length-to-width ratio was unchanged in these cells indicating that the cell size change was similar to that observed in physiologic hypertrophy (Hunter and Chien, 1999). Pathological cardiac hypertrophy is characterized by a prototypical change in gene expression patterns such as increased ANF, βMyHC,

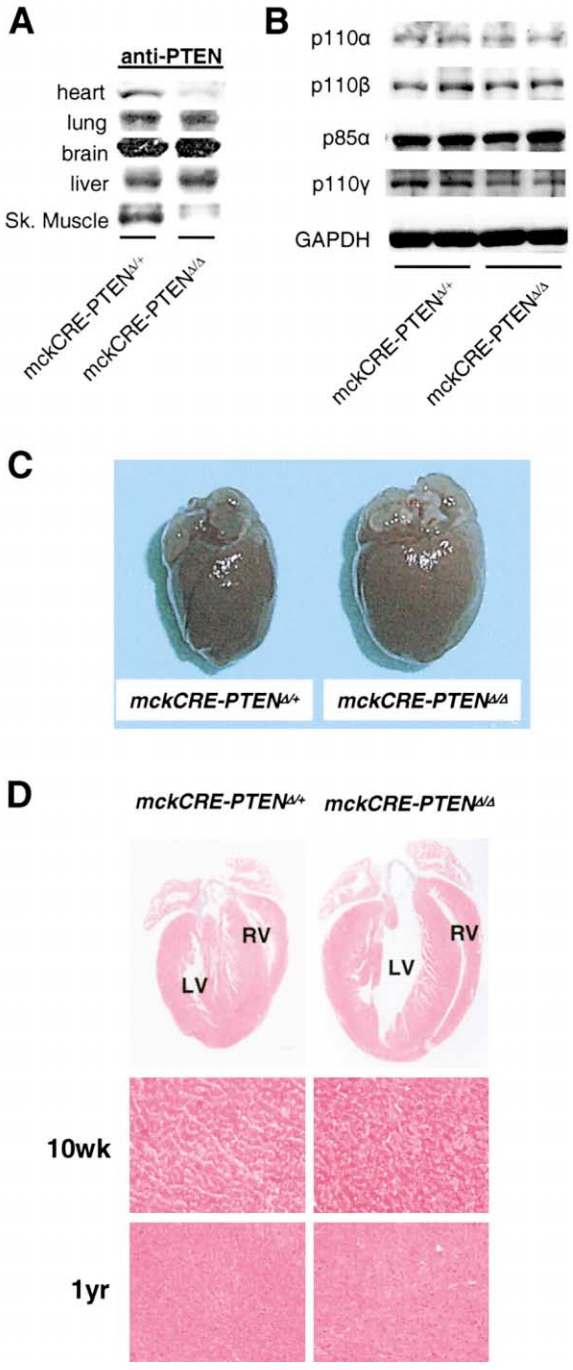

Figure 1. Cardiac Hypertrophy in PTEN Mutant Hearts

(A) Western blot analysis of proteins from different tissues of *mckCRE-PTEN*$^{\Delta/+}$ and *mckCRE-PTEN*$^{\Delta/\Delta}$ mice.

(B) Western blot analysis for p110α, p110β, p110γ, and p85 expression levels in total heart lysates from 2 representative *mckCRE-PTEN*$^{\Delta/+}$ and two *mckCRE-PTEN*$^{\Delta/\Delta}$ mice.

(C) Representative heart sizes of 10-week-old *mckCRE-PTEN*$^{\Delta/+}$ and *mckCRE-PTEN*$^{\Delta/\Delta}$ littermates.

(D) Heart sections from 10 week (upper and middle images) and 1 year (lower images) old *mckCRE-PTEN*$^{\Delta/+}$ and *mckCRE-PTEN*$^{\Delta/\Delta}$ mice. The middle and lower images show higher magnifications to detect interstitial fibrosis (trichrome). LV = left ventricle; RV = right ventricle.

BNP, and skeletal-actin expression, and a decrease in αMyHC (Hunter and Chien, 1999). However, no significant alterations in the expression profile of these hypertrophic genes were observed with the exception of an increase in βMyHC (Figures 2C and 2D). Thus, loss of PTEN in the myocardium induces hypertrophy without the typical pathological changes in the gene expression profiles or cardiac decompensation.

Activation of PI3K Signaling in PTEN-Deficient Hearts

Since PTEN antagonizes the action of PI3K, we analyzed whether the loss of PTEN in the hearts results in the activation of downstream targets of PI3K signaling (Downward, 1998). Loss of PTEN resulted in a significant increase in the basal phosphorylation state of AKT/PKB (Figures 2E and 2F). In addition, we found an increase in the phosphorylation of GSK3β and p70^{S6K}, both downstream targets of PI3K signaling (Figures 2E and 2F). No apparent changes in the basal activation of ERK1/ERK2 were observed between the mutant mckCRE-PTEN$^{\Delta/\Delta}$ mice and their mckCRE-PTEN$^{\Delta/+}$ and PTEN$^{+/+}$ littermates (Figures 2E and 2F). These data establish that loss of PTEN in cardiomyocytes results in increased PI3K signaling leading to activation and phosphorylation of multiple PI3K target molecules.

Loss of PTEN in the Heart Results in Decreased Cardiac Contractility

To further characterize the role of PTEN in mutant mckCRE-PTEN$^{\Delta/\Delta}$ mice, we analyzed the hearts using echocardiography. Consistent with the physiological cardiac hypertrophy, echocardiography of PTEN-deficient hearts revealed an increase in the anterior wall thickness and an increase of the left ventricle mass (LVM) at all ages analyzed (Figure 3A and Table 1). Moreover, the change in end diastolic dimension of the left ventricle (LVEDD) reflected this overall enlargement of PTEN-deficient heart. No difference in heart rate was detected in the PTEN-deficient hearts (Table 1).

Surprisingly, assessment of cardiac function by echocardiography revealed that mutant mckCRE-PTEN$^{\Delta/\Delta}$ mice exhibited a dramatic reduction in cardiac contractility characterized by decreased fractional shortening (FS), decreased velocity of circumferential fiber shortening (Vcfc), and reduced peak aortic outflow velocity (PAV; Figures 3B, 3C, and Table 1). To confirm the echocardiographic alterations, functional invasive hemodynamic measurements were performed. Our hemodynamic measurements showed that both dP/dT-max and dP/dT-min were markedly reduced in the PTEN mutant mice (Table 1), again indicating severe impairment of contractile heart function. Despite marked reductions in contractility at 10 weeks, there was no further decrease in the function of the PTEN-deficient hearts analyzed at 12 months of age (Table 1). In addition, there was no evidence of dilation, wall thinning, or tissue fibrosis in older animals (Figure 1D, Table 1). These data show that PTEN controls cardiomyocyte size and heart muscle contractility.

Increased Contractility in PI3Kγ Mutant Mice

The decrease in cardiac contractility found in the PTEN mutant hearts suggested that increased PI3K signaling

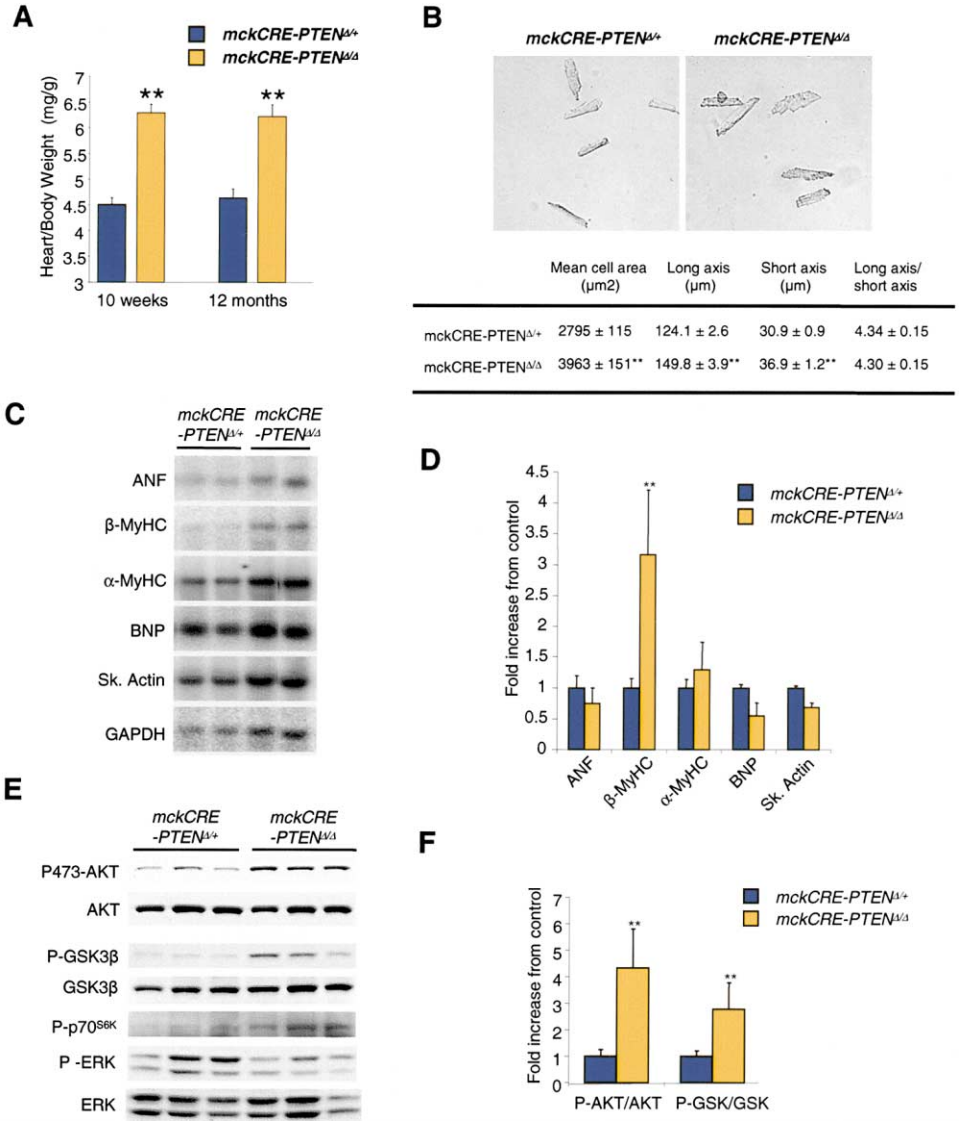

Figure 2. Cardiac Hypertrophy and PI3K Activation

(A) Quantitation of heart/body weight ratios from 10-week-old *mckCRE-PTEN*$^{\Delta/+}$ (n = 8) and *mckCRE-PTEN*$^{\Delta/\Delta}$ (n = 9) and 12 month old *mckCRE-PTEN*$^{\Delta/+}$ (n = 6) and *mckCRE-PTEN*$^{\Delta/\Delta}$ (n = 6) littermate mice.

(B) Increased cell sizes of cardiomyocytes isolated from 10-week-old *mckCRE-PTEN*$^{\Delta/\Delta}$ mice. Representative images of isolated cardiomyocytes and quantitation of cell sizes are shown. One hundred individual cells from three different mice were analyzed per group. ** $p < 0.01$ between genetic groups.

(C and D) Northern blot analysis and quantitation (mean values ± SEM) of cardiac hypertrophy markers. GAPDH expression levels were used as a loading control. Results from hearts isolated from 3 individual 10-week-old *mckCRE-PTEN*$^{\Delta/+}$ and 3 different, age-matched *mckCRE-PTEN*$^{\Delta/\Delta}$ littermate mice are shown.

(E and F) Increased AKT/PKB, GSK3β, and p70^{S6K} phosphorylation in total heart extracts from 10-week-old *mckCRE-PTEN*$^{\Delta/\Delta}$ mice. Western blot of the expression of phospho-AKT/PKB, phospho-GSK3β, phospho-p70^{S6K}, phospho-ERK1/2, and their respective loading controls. Densitometric quantitation of phospho-AKT/PKB and phospho-GSK3β levels relative to total cellular AKT/PKB and GSK3β. Mean values ± SEM are representative of 3 independent experiments. ** $p < 0.01$ between genetic groups.

serves not only to increase cell size in the heart but to also suppress basal heart function. Neither the p110α dominant-negative nor p110α constitutively active heart specific transgenic animals showed any alteration in heart function (Shioi et al., 2000) suggesting that the effect on contractility is mediated by PI3K isoforms other than PI3Kα. Since several GPCR signaling pathways, including adrenergic receptors (Rockman et al., 2002), are important mediators of cardiac function, we hypothesized that the decreased heart function in PTEN mutant mice is mediated by PI3Kγ. We observed p110γ protein expression in total heart extracts of mice (Figure 1B) and in isolated cardiomyocytes (Figure 3D). Loss of p110γ expression does not alter the expression levels of p85, p110α, and p110β (Figure 3E). Moreover, p85 associated PI3K activity in cardiomyocytes was comparable between p110γ$^{-/-}$ and wild-type littermates using in vitro lipid kinase assays (not shown). There was also no ap-

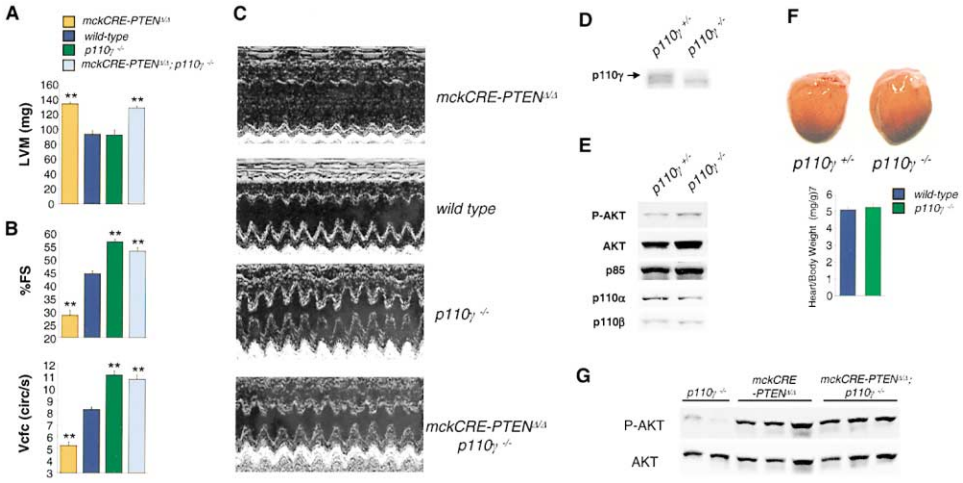

Figure 3. Modulation of Cardiac Contractility in PTEN and p110γ Mutant Hearts

(A) Left ventricular mass (LVM; mean values ± SEM) in hearts from 10-week-old *mckCRE-PTEN*$^{\Delta/\Delta}$ (n = 8), *wild-type* (n = 7), *p110*$\gamma^{-/-}$ (n = 7), and *mckCRE-PTEN*$^{\Delta/\Delta}$ *p110*$\gamma^{-/-}$ (n = 8) mice. ** $p < 0.01$ between genetic groups.

(B) Percent fractional shorting (% FS) and velocity of circumferential fiber shortening (Vcfs) in 10-week-old *mckCRE-PTEN*$^{\Delta/\Delta}$, *wild-type*, *p110*$\gamma^{-/-}$, and *mckCRE-PTEN*$^{\Delta/\Delta}$ *p110*$\gamma^{-/-}$ double-mutant mice. Mean values ± SEM were determined by echocardiography. ** $p < 0.01$ between groups.

(C) M-mode echocardiographic images of contracting hearts in 10-week-old *mckCRE-PTEN*$^{\Delta/\Delta}$, *wild-type*, *p110*$\gamma^{-/-}$, and *mckCRE-PTEN*$^{\Delta/\Delta}$ *p110*$\gamma^{-/-}$ mice. Note that contracting hearts in *mckCRE-PTEN*$^{\Delta/\Delta}$ *p110*$\gamma^{-/-}$ double mutants are similar to that of *p110*$\gamma^{-/-}$ mice.

(D) Western blot analysis for p110γ expression in control and p110γ deficient isolated cardiomyoctes. Note the smaller non-specific band.

(E) Western blotting for phosphorylated-AKT/PKB, total AKT/PKB protein, p85, p110α, and p110β protein expression in total heart extracts.

(F) Representative heart sizes and heart/body weight ratios of 10 week old *p110*$\gamma^{+/-}$ and *p110*$\gamma^{-/-}$ littermates. Similar data, i.e, no change in heart size, were obtained at 6 and 12 months of age.

(G) Western blot analysis of AKT/PKB phosphorylation and total AKT/PKB protein levels in hearts from individual *p110*$\gamma^{-/-}$, *mckCRE-PTEN*$^{\Delta/\Delta}$ and *mckCRE-PTEN*$^{\Delta/\Delta}$ *p110*$\gamma^{-/-}$ double-mutant mice.

parent difference in the expression or phosphorylation of AKT/PKB (Figure 3E). Mice deficient for p110γ were found to have no alteration in heart size or left ventricle mass (LVM) and displayed normal heart rates (Figures 3A, 3F, and Table 1). No structural alterations were observed in the hearts of p110$\gamma^{-/-}$ mice using histological analyses and there were no changes in the gene expression profiles of the cardiac hypertrophy markers ANF, βMyHC, BNP, skeletal-actin, and αMyHC. Thus, whereas loss of PTEN results in cardiac hypertrophy, PI3K has no role in the control of basal cardiomyocyte size.

Intriguingly, the hearts of p110γ deficient mice displayed a marked enhancement in contractility as assessed by increased fractional shortening (FS), Vcfc, and peak aortic outflow velocity (PAV; Figures 3B, 3C, and Table 1). Hemodynamic measurements confirmed the increased heart contractility in p110$\gamma^{-/-}$ mice (Table 1). Telemetry analysis of blood pressure in conscious mice revealed normal blood pressure in p110$\gamma^{-/-}$ mice (not shown). In addition, plasma epinephrine and norepinephrin levels were not altered in p110$\gamma^{-/-}$ mice compared to controls [norepinephrin (59.63 ± 9.99 in wild-type (n = 6) versus 61.28 ± 8.82 in p110$\gamma^{-/-}$ mice (n = 6), and epinephrin (4.65 ± 0.80 in wild-type (n = 6) versus 4.28 ± 0.55 in p110$\gamma^{-/-}$ mice (n = 6)].

To determine if there are any long-term effects of this increase in cardiac function in p110γ deficient mice, we analyzed heart function by echocardiography in 1-year-old mice. Similar to that observed in younger mice, there remained an increase in cardiac contractility [fractional shortening (48.49 ± 0.76 in wild-type (n = 6) versus 55.16 ± 0.33 in p110$\gamma^{-/-}$ mice (n = 6), and Vcfc (8.65 ± 0.20 in wild-type (n = 6) versus 10.86 ± 0.17 in p110$\gamma^{-/-}$ mice (n = 6)]. To ensure that the increase in cardiac contractility observed in the p110γ was due to the disruption of the gene and not an aberrant gene targeting event, we analyzed heart function in a second independently generated mouse line deficient for p110γ (Hirsch et al., 2000). All alterations in heart functions analyzed were similar between the two independent p110γ deficient mouse lines. Specifically, the second p110γ mouse line (Hirsch et al., 2000) had increased contractility as assessed by fractional shortening [48.07 ± 0.68 in wild-type (n = 6) versus 56.47 ± 0.87 in p110$\gamma^{-/-}$ mice (n = 6), and Vcfc (8.62 ± 0.16 in wild-type (n = 6) versus 11.35 ± 0.28 in p110$\gamma^{-/-}$ mice (n = 6)]. Moreover, hypercontractility persisted (Vcfc: 8.65 ± 0.2 in wild-type versus 10.86 ± 0.17 in p110$\gamma^{-/-}$ mice; n = 6; $p < 0.01$) and there was no evidence of cardiac hypertrophy or increased myocardial fibrosis in 1-year-old mice (not shown). Thus, loss of PI3Kγ results in a marked increase in cardiac contractility.

PI3Kγ Mediates Reduction of Heart Function in PTEN-Deficient Hearts

The alterations in heart muscle contractility in p110γ− and PTEN mutant hearts were exactly opposite, that is loss of PTEN resulted in decreased heart functions whereas loss of p110γ leads to a marked enhancement in cardiac contractility. To determine if the role of PTEN in regulating cell size and heart function could be geneti-

Table 1. Heart Functions of Mutant Mice

	10 Weeks		12 Months					
	mckCRE-PTEN$^{\Delta/+}$ (wildtype)	*mckCRE-PTEN$^{\Delta/\Delta}$*	*mckCRE-PTEN*	*mckCRE-PTEN$^{\Delta/\Delta}$*	*p110$\gamma^{-/-}$*	*mckCRE-PTEN$^{\Delta/\Delta}$ p110$\gamma^{-/-}$*	*DN-p110α*	*mckCRE-PTEN$^{\Delta/\Delta}$ DN-p110α*
	n=7	n=7	n=6	n=6	n=7	n=8	n=4	n=4
Heart Rate, bpm	518 ± 13	545 ± 19	545 ± 9	529 ± 18	486 ± 25	535 ± 11	522 ± 7	533 ± 7
AW, mm	0.67 ± 0.03	**0.74 ± 0.03**[b]	0.70 ± 0.03	**0.84 ± 0.02**[b]	0.70 ± 0.02	**0.80 ± 0.01**[b]	**0.61 ± 0.01**[a]	**0.57 ± 0.03**[a]
LVEDD, mm	4.00 ± 0.07	**4.35 ± 0.15**[a]	4.10 ± 0.05	4.32 ± 0.15	3.99 ± 0.11	**4.12 ± 0.04**[a]	3.87 ± 0.09	3.85 ± 0.14
LVESD, mm	2.20 ± 0.04	**3.11 ± 0.14**[b]	2.24 ± 0.05	**2.92 ± 0.15**[a]	**1.74 ± 0.06**[b]	**1.94 ± 0.06**[a]	2.10 ± 0.07	**2.57 ± 0.07**[b]
LVM, mg	97.39 ± 2.82	**134.04 ± 2.64**[b]	103.57 ± 4.87	**142.93 ± 4.59**[b]	92.22 ± 6.75	**128.87 ± 2.59**[a]	**83.18 ± 1.23**[a]	**83.55 ± 1.42**[a]
% FS	44.97 ± 0.68	**28.39 ± 1.90**[b]	44.50 ± 1.28	**32.86 ± 1.26**[b]	56.50 ± 0.95[b]	**52.96 ± 1.39**[b]	45.62 ± 0.82	**32.26 ± 0.80**[b]
Vcfc, circ/s	8.71 ± 0.10	**5.26 ± 0.30**[b]	9.23 ± 0.18	**6.41 ± 0.23**[b]	**11.15 ± 0.34**[b]	**10.78 ± 0.36**[a]	9.39 ± 0.22	**6.51 ± 0.21**[b]
PAV, m/s	0.940 ± 0.024	**0.887 ± 0.023**[a]	0.826 ± 0.029	**0.697 ± 0.019**[a]	**1.017 ± 0.052**[b]	**1.116 ± 0.070**[b]	0.886 ± 0.044	0.830 ± 0.024
dP/dT-max	+6045 ± 148	**+4077 ± 243**[b]			**+9202 ± 473**[b]			
dP/dT-min	−5274 ± 251	**−3731 ± 158**[b]			**−8036 ± 500**[b]			

[a] $p < 0.05$ versus wild-type mice.
[b] $p < 0.01$ versus wild-type mice.
Bpm = heart beats per minute; AW = anterior wall thickness; LVEDD = left ventricle and diastolic dimension; LVESD = left ventricle end systolic dimension; LVM = left ventricular mass; % FS = percent fractional shortening; Vcfc = Velocity of circumferential fiber shortening; PAV = peak aortic outflow velocity. dP/dT max = maximum 1st derivative of the change in left ventricular pressure/time; dP/dT min = minimum 1st derivative of the change in left ventricular pressure/time

cally uncoupled, we generated mice deficient for both p110γ and PTEN in the heart. Hearts from mckCRE-PTEN$^{\Delta/\Delta}$ p110$\gamma^{-/-}$ double-mutant mice were significantly enlarged as compared to wild-type and p110$\gamma^{-/-}$ mutant mice (Figure 3A, Table 1). The extent of cardiac hypertrophy in mckCRE-PTEN$^{\Delta/\Delta}$ p110$\gamma^{-/-}$ double-mutant mice was similar to that observed for hearts from mckCRE-PTEN$^{\Delta/\Delta}$ single mutants (Figure 3A). Histologically, hearts from mckCRE-PTEN$^{\Delta/\Delta}$ p110$\gamma^{-/-}$ double-mutant mice were also similar to that of mckCRE-PTEN$^{\Delta/\Delta}$ single mutant mice. Importantly, similar to PTEN-deficient hearts, AKT/PKB was hyperphosphorylated in the hearts of mckCRE-PTEN$^{\Delta/\Delta}$ p110$\gamma^{-/-}$ double-mutant mice (Figure 3G). Thus, loss of PI3Kγ in PTEN-deficient hearts has no affect on the increased AKT/PKB phosphorylation and does not rescue the cardiac hypertrophy phenotype.

However, unlike PTEN-deficient hearts, mckCRE-PTEN$^{\Delta/\Delta}$ p110$\gamma^{-/-}$ double-mutant hearts were found to be hypercontractile, as assessed by increased fractional shortening (FS), Vcfc, and peak aortic outflow velocity (PAV; Figures 3B, 3C, and Table 1). These improved heart functions were similar to that of p110γ single mutant hearts. These data show that the defect in cardiac contractility seen in the PTEN-deficient hearts is dependent on the PI3Kγ signaling pathway. Importantly, PTEN regulated hypertrophy can be genetically uncoupled from the cardiac contractility changes mediated by PTEN-PI3Kγ.

Reversal of Cardiac Hypertrophy in PTEN-Deficient Hearts by a Dominant-Negative p110α Transgene

The increase in cell size found in PTEN-deficient hearts strongly resembles that seen in transgenic mice for heart specific constitutively active p110α that couples to receptor tyrosine kinases (Shioi et al., 2000). Furthermore, mice transgenic for heart-specific dominant-negative p110α (DN-p110α) have smaller than normal heart size. We therefore generated mice deficient for PTEN in the hearts and overexpressing the heart specific DN-p110α transgene. Hearts of mckCRE-PTEN$^{\Delta/\Delta}$;DN-p110α mice displayed a reduction in heart size similar to that seen in single DN-p110α transgenic mice (Figures 4A and 4B). The presence of the DN-p110α transgene also correlated with a decrease in the basal level of AKT/PKB activation in the absence or presence of a functional PTEN gene (Figure 4C). However, whereas overexpression of DN-p110α on a wild-type background affects heart size but has no apparent effect on heart function, hearts from mckCRE-PTEN$^{\Delta/\Delta}$;DN-p110α displayed a marked decrease in contractility (Figures 4D, 4E, and Table 1). Taken together, these data show that PI3Kα signaling modulates basal cell size of cardiomyocytes while PI3Kγ signaling controls basal cardiac contractility.

PI3Kγ and PTEN Control Contractility in Single Cells

To further analyze these in vivo contractility defects, we elucidated whether loss of PTEN and PI3Kγ can affect contractility of a single adult cardiomyocyte in vitro. In agreement with both the in vivo echocardiographic and

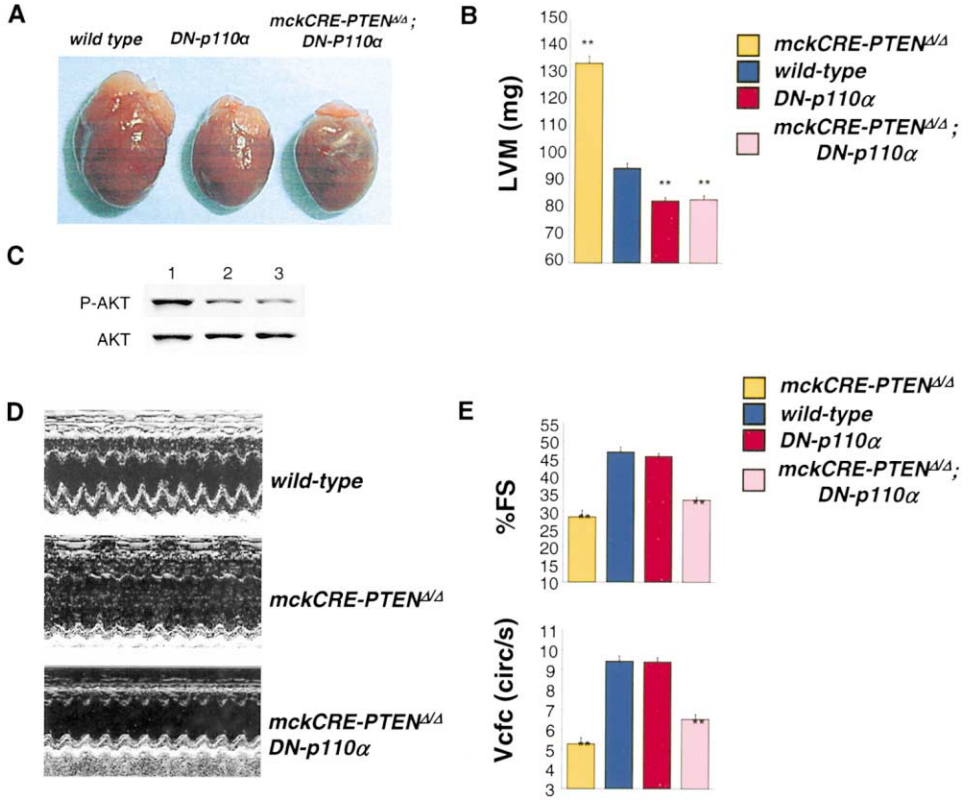

Figure 4. Heart Sizes and Functions in *mckCRE-PTEN*$^{\Delta/\Delta}$ *DN-p110*α Mice

(A) Representative heart sizes of 10-week-old *wild-type, DN-p110*α, and *mckCRE-PTEN*$^{\Delta/\Delta}$ *DN-p110*α littermates.

(B) Left ventricular mass (LVM; mean values $\pm$ SEM) in hearts from 10 week old *mckCRE-PTEN*$^{\Delta/\Delta}$ (n = 8), *wild-type* (n = 6), *DN-p110*α (n = 4), and *mckCRE-PTEN*$^{\Delta/\Delta}$ *DN-p110*α double transgenic (n = 4). ** $p < 0.01$ between genetic groups.

(C) Western blot analysis of AKT/PKB phosphorylation and total AKT/PKB protein levels in hearts from *wild-type* (lane 1), *DN-p110*α single transgenic (lane 2), and *mckCRE-PTEN*$^{\Delta/\Delta}$ *DN-p110*α double-transgenic (lane 3) mice.

(D) M-mode echocardiographic images of contracting hearts in 10-week-old *wild-type*, *mckCRE-PTEN*$^{\Delta/\Delta}$, and *mckCRE-PTEN*$^{\Delta/\Delta}$ *DN-p110*α double-transgenic mice.

(E) Percent fractional shorting (% FS) and velocity of circumferential fiber shortening (Vcfs) in 10-week- old *mckCRE-PTEN*$^{\Delta/\Delta}$ (n = 8), *wild-type* (n = 6), *DN-p110*α (n = 4), and *mckCRE-PTEN*$^{\Delta/\Delta}$ *DN-p110*α double-transgenic (n = 4) mice. Values (mean $\pm$ SEM) were determined by echocardiography. ** $p < 0.01$ between groups.

hemodynamic data, it was found that PTEN deficient cardiomyocytes display a reduction in contractility as determined by a reduction in percent cell shortening and positive and negative dL/dTs as compared to wild-type cardiomycoytes (Figures 5A and 5B; Table 2). Conversely, p110γ deficient myocytes displayed an increase in contractility (Figures 5A and 5B; Table 2). Cardiomyocytes deficient for both PTEN and p110γ display increased contractility despite the hypertrophy present in these cells (Figures 5A and 5B; Table 2). Moreover, treatment of wild-type myocytes with the PI3K inhibitor LY294002 lead to a significant increase in cardiomyocyte contractility. In p110γ deficient cardiomyocytes, addition of LY294002 had no effect on the already increased contractility (Figure 5B; Table 2). These in vitro data show that independent of exogenous agonists PTEN and PI3Kγ control basal cardiomyocyte contractility within a single cell.

PI3Kγ Modulates Baseline cAMP Levels in Cardiomyocytes

One intriguing aspect of the in vitro contractility data is that there was a significant increase in the rate of relaxation in p110γ deficient cardiomyocytes compared to control cells despite a marked increase in peak contraction (Table 2). Cardiac relaxation is modulated via cAMP dependent pathways, where cAMP activates PKA, which then inhibits phospholamban (PLB) leading to increased sarcaplasmic reticulum calcium ATPase (SERCA) activity (Brittsan and Kranias, 2000). Moreover, it has previously been shown in vascular smooth muscle cells that pharmacological inhibition of PI3K can lead to increases in cAMP levels (Komalavilas et al., 2001). To determine if alterations in cAMP levels may also be contributing to the phenotype observed here, we measured baseline cAMP levels in isolated myocytes. In unstimulated PTEN-deficient cardiomyocytes, cAMP levels were significantly reduced (Figure 5C). Conversely, an increase in cAMP levels was detected in isolated cardiomyocytes deficient for p110γ (Figure 5C). Importantly, treatment of PTEN-deficient and wild-type cardiomyocytes with the PI3K inhibitor Wortmannin resulted in a marked increase of cAMP to levels observed in p110γ deficient cells (Figure 5C). Induction of cAMP production in response to the adenylate cyclase agonist forskolin was comparable among all genotypes ana-

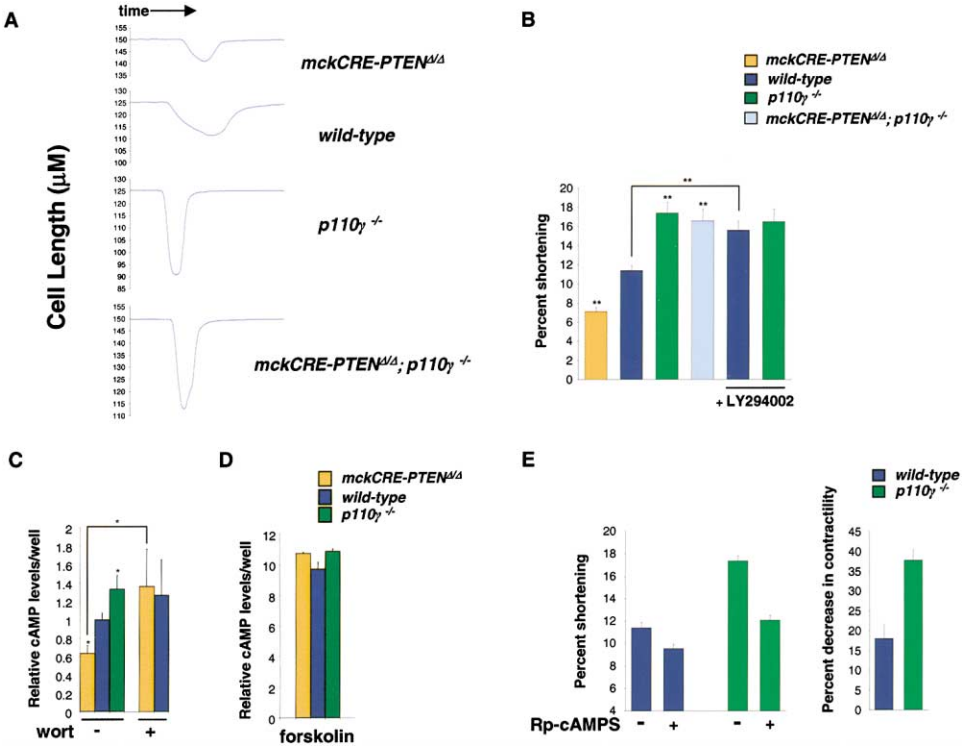

Figure 5. Single Cell Contractility and cAMP Production

(A and B) Basal contractility of single cardiomyocytes isolated from *mckCRE-PTEN*$^{\Delta/\Delta}$, *wild-type*, *p110*$\gamma^{-/-}$, and *mckCRE-PTEN*$^{\Delta/\Delta}$ *p110*$\gamma^{-/-}$ double-mutant mice. In (A), representative contractions from single cells are shown. In (B), mean percentage shortening (± SEM) of at least 15 different single cells from 3 different hearts per genotype are shown in the presence and absence of the PI3K inhibitor LY294002 [30 μM]. ** $p < 0.01$ between groups.

(C) Basal cAMP levels (mean ± SEM) in purified cardiomyocytes from *mckCRE-PTEN*$^{\Delta/\Delta}$, *wild-type*, and *p110*$\gamma^{-/-}$ mice (n = 4 for each genotype). Samples were either left untreated (−) or treated with wortmannin (wort, +). * $p < 0.05$ between groups.

(D) Activation of adenylate cyclase via forskolin [25 μM] increases the levels of cAMP production (mean ± SEM) in *mckCRE-PTEN*$^{\Delta/\Delta}$, *wild-type,* and *p110*$\gamma^{-/-}$ cardiomyocytes to a similar extent.

(E) Inhibition of cAMP dependent functions via Rp-cAMPS [25 μM] reduces cell shorting (contractility) in single *wild-type* and *p110*$\gamma^{-/-}$ cardiomyocytes. Mean values (± SEM) of percent shortening in the presence of Rp-cAMPS (left image) and percent decrease in contractility using Rp-cAMPS are shown. ** $p < 0.01$ between groups.

lyzed (Figure 5D) indicating that the basal machinery for cAMP production is operational in all genotypes. These genetic data show that PI3Kγ and PTEN modulate cAMP production in cardiomyocytes.

To determine if these alterations in cAMP levels contribute to altered contractility, we measured contractility in single cells following blockade of cAMP-dependent activation of downstream targets using Rp-cAMP. In wild-type adult mouse cardiomyocytes, treatment with Rp-cAMP lead to a marked decrease in contractility (Figure 5E; Table 2). Importantly, treatment of p110γ deficient cardiomyocytes with the cAMP blocker lead to a greater reduction in contractility as compared to wild-type cells such that the difference in the resultant

Table 2. Contractility of Isolated Single Cardiomyocytes

	Wildtype	*mckCRE-PTEN*$^{\Delta/\Delta}$	*p110*$\gamma^{-/-}$	*mckCRE-PTEN*$^{\Delta/\Delta}$ *p110*$\gamma^{-/-}$	*Wildtype* (*LY294002*) (*30μM*)	*p110*$\gamma^{-/-}$ (*LY294002*) (*30μM*)	*Wildtype* (*Rp-CAMPs*) (*25μM*)	*p110*$\gamma^{-/-}$ (*Rp-CAMPs*) (*25μM*)
Resting Length, μm	121.7 ± 3.1	**146.7 ± 2.9**[a]	123.6 ± 3.2	**147.3 ± 2.4**[a]	123.8 ± 2.1	124.1 ± 3.4	120.6 ± 2.6	122.1 ± 2.2
% Shortening	11.4 ± 0.51	**7.1 ± 0.43**[a]	**17.4 ± 1.1**[a]	**16.6 ± 1.2**[a]	**15.6 ± 0.97**[a]	**16.5 ± 1.3**[a]	**9.58 ± 0.37**[a]	**12.1 ± 0.41**[b]
+dL/dT, μm/s	339 ± 17.2	**224 ± 14.3**[a]	**797 ± 45**[a]	**723 ± 42**[a]	**503 ± 22.5**[a]	**717 ± 53**[a]	**278 ± 12.3**[a]	**496 ± 21.3**[b]
−dL/dT, μm/s	358 ± 18.1	**242 ± 16.4**[a]	**960 ± 56**[a]	**889 ± 58**[a]	**521 ± 25.8**[a]	**912 ± 63**[a]	**289 ± 17.2**[a]	**579 ± 31.6**[a]
TPS, ms	55.3 ± 3.2	49.4 ± 3.8	48.7 ± 2.2	50.2 ± 2.4	50.3 ± 2.9	53.3 ± 3.1	54.7 ± 2.8	53.1 ± 2.6
T90R, ms	71.9 ± 3.6	76.7 ± 4.5	**54.7 ± 2.8**[a]	**51.3 ± 2.6**[a]	**50.1 ± 2.8**[a]	**50.5 ± 2.5**[a]	76.9 ± 3.2	**68.8 ± 3.7**[b]

[a] $p < 0.01$ versus wildtype cells.

[b] $p < 0.01$ versus untreated p110$\gamma^{-/-}$.

Mean ± SEM are shown; n = 15 cells from 3 hearts for each group. +dL/dT max = maximum 1st derivative of the change in cell length/time; −dL/dT = minimum 1st derivative of the change in cell length/time; TPS=time to peak shortening; T90R=time to 90% relaxation.

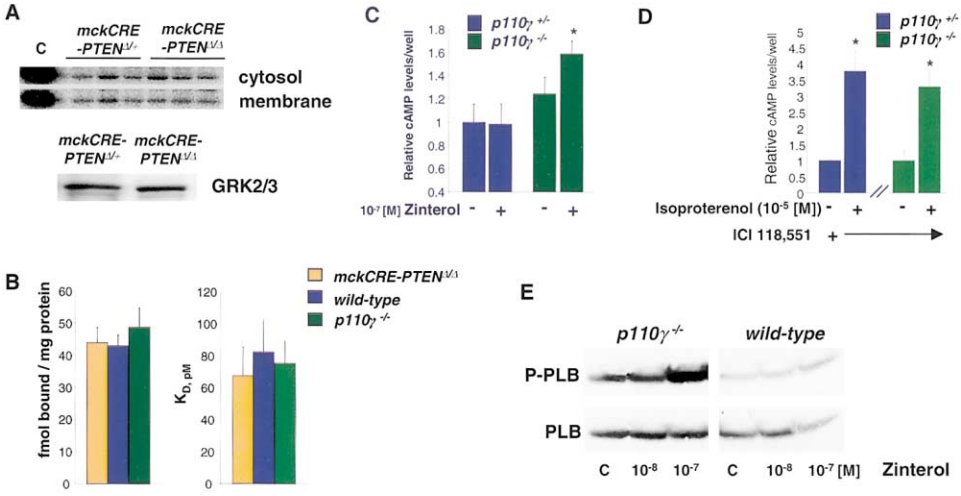

Figure 6. PI3Kγ and β-Adrenergic Signaling

(A) GRK kinase activities from fractionated heart lysates from individual *mckCRE-PTEN*$^{\Delta/+}$ and *mckCRE-PTEN*$^{\Delta/\Delta}$ mice were determined using in vitro kinase assays and rhodopsin as substrate. Since GRKs are recruited to membranes, data from cytosolic and membrane fractions are shown. C = control using recombinant GRK2. The lower image shows a Western blot of total GRK2/3 expression levels in the hearts.

(B) β-AR densities were determined using ICYP as a ligand as described in Experimental Procedures (n = 7 for *wild-type*; n = 5 for *mckCRE-PTEN*$^{\Delta/\Delta}$; and n = 5 for *p110*$\gamma^{-/-}$).

(C) Induction of cAMP production in response to the selective β2-adrenergic receptor agonist zinterol. Note that zinterol has no detectable effect on β2-AR induced cAMP levels in *wild-type* cardiomyocytes (n = 5) but significantly increases cAMP levels in *p110*$\gamma^{-/-}$ cardiomyocytes (n = 5). * $p < 0.05$ between groups.

(D) Induction of cAMP production in response to β1-adrenergic receptor stimulation. Both *wild-type* (n = 4) and *p110*$\gamma^{-/-}$ cardiomyocytes (n = 4) respond equally to isoproterenol. β2-AR were blocked with pretreatment of ICI 118,551.

(E) Western blot analysis of phosphorylated phospholamban (P-PLB) and total phospholamban (PLB) in *wild-type* and *p110*$\gamma^{-/-}$ cardiomyocytes in response to different concentrations of the selective β2-AR agonist zinterol. C = control. Note the increased phosphorylation of PLB in unstimulated *p110*$\gamma^{-/-}$ cardiomyocytes that mirrors increased basal cAMP levels in these cells. One representative experiment is shown.

contractility of wild-type and p110γ deficient cells treated with Rp-cAMP was greatly reduced compared to untreated cells (Figure 5E; Table 2). In addition, the rate of relaxation in p110γ deficient cardiomyocytes treated with Rp-cAMP was reduced to wild-type levels (Table 2). These data indicate that alterations in baseline cAMP levels contribute to the increased contractility in p110$\gamma^{-/-}$ hearts.

PI3Kγ and β-Adrenergic Signaling

It has been previously shown that PI3Kγ can bind to GPCR-kinase 2 (GRK2; Naga Prasad et al., 2001a), a kinase that mediates desensitization of GPCRs like β-adrenergic receptors (β-AR; Lefkowitz, 1998). Thus, we speculated that β-adrenergic signaling may be affected in p110$\gamma^{-/-}$ hearts, and that alterations of PI3K activity may affect GRK activity and/or β-AR expression. Using an in vitro kinase assay, GRK activity in both cytosolic and membrane-associated fractions of PTEN-deficient hearts was comparable to that of control hearts (Figure 6A). Total protein levels of GRK2 were also comparable (Figure 6A). Radiolabeled ligand binding assays showed that there is also no detectable difference in the density of β-AR receptors or their affinity for the β-AR ligand ICYP in the PTEN- or p110γ-deficient hearts as compared to wild-type mice (Figure 6B). These data imply that changes in contractility of PTEN and p110γ-deficient hearts are not due to alterations in baseline β-adrenergic receptor levels or the modulation of GRK activity.

The G protein coupled β_2-adrenergic receptors (β_2-AR) are linked to both Gαs and Gαi G-proteins that can either increase (Gαs) or decrease (Gαi) cAMP levels and heart muscle contractility (Kuznetsov et al., 1995; Xiao et al., 1999; Rockman et al., 2002). To determine if PI3Kγ can modulate cAMP production following GPCR stimulation, we purified neonatal cardiomyocytes from both wild-type and p110$\gamma^{-/-}$ hearts and stimulated these cells with the β2-AR selective agonist zinterol. As described previously for adult rat myocytes (Kuznetsov et al., 1995), stimulation of the β2-AR had no affect on cAMP levels in wild-type mouse cardiomyoctes. By contrast, selective stimulation of the β2-AR in p110$\gamma^{-/-}$ cardiomyocytes resulted in a marked increase in cAMP levels (Figure 6C). Conversely, stimulation of β1-AR receptors resulted in a similar increase in cAMP levels in both wild-type and p110γ-deficient cardiomyocytes demonstrating selectivity for the action of PI3Kγ on cAMP production (Figure 6D).

In cardiomyocytes, increased cAMP levels result in enhanced contractility via activation of PKA and subsequent phosphorylation of phospholamban (PLB) in the sarcoplasmic reticulum (Brittsan and Kranias, 2000). Similar to cAMP production, no alteration of PLB phosphorylation could be detected in wild-type cells upon stimulation with the β2-AR agonist zinterol (Figure 6E). However, when *p110*$\gamma^{-/-}$ cardiomyocytes were stimulated with the same β2-AR agonist, a dose dependent increase in PLB phosphorylation was observed. Thus, in addition to its role in baseline cardiac contractility,

loss of p110γ expression releases the inhibition of the β2-AR thereby permitting receptor-induced cAMP production and subsequent PLB-phosphorylation.

Discussion

We elucidated the roles of PI3K-PTEN signaling in cardiac hypertrophy and heart functions in PTEN-heart muscle specific mutant mice, p110γ knockout, dominant-negative p110α transgenic mice, and double-mutant mice. We show that the tyrosine kinase-receptor p110α-PTEN pathway is a critical regulator of cardiac cell size. Intriguingly, our data revealed that the PTEN-PI3Kγ signaling pathway regulates heart muscle contractility via GPCRs. This contractility phenotype is present in single cardiomyocytes and dependent on cAMP signaling. PI3Kγ regulates cardiac function by negatively regulating cAMP levels and phospholamban phosphorylation upon β_2-adrenergic receptor stimulation. These data show that the tumor suppressor PTEN has an important in vivo role in GPCR signaling and that PTEN and PI3Kγ signaling control heart function.

PTEN and Heart Muscle Size

The cardiac hypertrophy in PTEN deficient hearts is similar to that in mice overexpressing a constitutively active p110α transgene in the heart (Shioi et al., 2000). Like these transgenic mice, the hypertrophy found in PTEN deficient hearts displayed features characteristic of physiological hypertrophy, such as increase in both the length and width of the myocytes, no fibrotic changes, and no decompensation into dilated cardiomyopathy (Hunter and Chien, 1999). The reversal of heart size in the PTEN deficient hearts that expressed a dominant-negative PI3Kα transgene indicates that it is this isoform of PI3K that modulates basal cell size in cardiomyocytes. Moreover, it does not appear that any other PI3K isoform can compensate for the loss of PI3Kα function in vivo. It should be pointed out that it is possible that this transgene interferes with not only p110α, but also p110β and p110δ, as all of these require p85 activity which is likely sequestered as a result of the transgene expression. Nevertheless, these data does show a differential action of class Ia and class Ib PI3Ks, as it is unlikely that this transgene interferes with p110γ function. This is further supported by the absence of any observable alteration in cardiac contractility in mice expressing the DN-p110α transgene.

Previously, PI3K signaling has been implicated in cell size regulation in other tissues and organisms such as *Drosophila* (Scanga et al., 2000). Mice deficient for $p70^{S6K}$ have reduced body size due to a reduction in cell size (Shima et al., 1998). Recently, brain specific disruptions of PTEN have been reported which result in the increase in neuronal cell size (Backman et al., 2001). Moreover, transgenic expression of activated AKT/PKB in mouse heart leads to a hypertrophic phenotype and this phenotype can be inhibited with a DN-p110α transgene (Shioi et al., 2002; Matsui et al., 2002). This is consistent with our data on the differential modulation of AKT/PKB phosphorylation in PTEN but not PI3Kγ mutant hearts. Thus, it appears that AKT/PKB and $p70^{S6K}$ signaling plays an important role in the regulation of basal cardiomyocyte size in vivo.

Our results show that PI3Kγ has no role in the homeostatic control of cardiomyocyte cell size. Yet many agonists used to induce PI3K-dependent cardiomyocyte hypertrophy in vitro are GPCR agonists (Rabkin et al., 1997; Schluter et al., 1999). Moreover, PI3Kγ is activated in pressure overload induced hypertrophy in vivo (Naga Prasad et al., 2000), implying a role for PI3Kγ in agonist-induced cardiac hypertrophy. Thus, it will be interesting to determine if PI3Kγ may play a role in agonist-induced hypertrophy in vivo following stimulation of GPCRs.

Regulation of Heart Muscle Contractility by PI3Kγ and PTEN

While the cardiac hypertrophy observed in the PTEN deficient hearts was similar to that seen in p110α transgenic mice, PTEN deficient hearts surprisingly also displayed a dramatic decrease in cardiac contractility. Conversely, PI3Kγ deficient hearts exhibited an increase in cardiac contractility. These data reveal that PI3Kγ-PTEN signaling control heart muscle function in vivo. Importantly, the data presented here show that PI3Kγ can modulate contractility in the absence of exogenous agonists. These contractility changes are at least in part mediated by alteration in cAMP levels.

An interesting conceptual issue arises from this work: how do these different PI-3 kinases trigger distinct cellular responses? If the function is at the level of lipid phosphorylation, are the lipids different or do they have different localization? For instance, both the spatial and temporal organization of signaling complexes is crucial for the specificity of outcomes (Milligan and White, 2001). Or is it the proposed protein kinase activity of these enzymes? While both PI3K and PTEN have been shown to possibly act on protein substrates in vitro, no common protein substrates have been identified (Bondeva et al., 1998; Tamura et al., 1998). Thus, most likely the phenotypes observed here are due to the lipid kinase/phosphatase activity of these enzymes. Hearts deficient in both PTEN and PI3Kγ also displayed increased cardiac contractility indicating that increased PIP3 generated via PI3Kγ causes the decrease in cardiac contractility seen in the PTEN deficient hearts. Moreover, it is possible that the different receptors recruit different downstream targets for the same phospholipids.

β2 adrenergic receptors are coupled to both Gαs and Gαi signaling (Rockman et al., 2002). The opposing effects of these two G protein subunits result in no global net effect on cardiac contractility or cAMP production upon receptor stimulation (Kuznetsov et al., 1995; Xiao et al., 1999). It has been shown, however, that if the Gαi subunit is inhibited, a Gαs response and an increase in myocyte contractility ensues (Xiao et al., 1999). Our results indicate that loss of PI3Kγ in heart muscle cells relieves an inhibition resulting in cAMP production and PLB phosphorylation upon β2 AR agonist stimulation consistent with an inhibition of Gαi. In this scenario, loss of PI3Kγ would result in a lack of Gαi cAMP inhibition and a subsequent increase in cAMP levels and PLB phosphorylation resulting in the inhibition of PLB and increased SERCA function effectively enhancing contractility (Zvaritch et al., 2000; Frank and Kranias, 2000).

Additional molecular mechanisms controlling cAMP levels and PLB phosphorylation in a PTEN-PI3Kγ dependent manner cannot be excluded.

In heart failure, β1-AR densities decrease leading to a greater prominence of β2 adrenergic signaling (Naga Prasad et al., 2001b). Furthermore, it has been shown that increased PLB activity is a critical regulator of decreased contractility in dilated cardiomyopathy (Minamisawa et al., 1999). It is not known if PI3Kγ is upregulated in heart failure; however, it is known that p110γ expression can be induced in pressure overload hypertrophy (Naga Prasad et al., 2000). Thus, in the presence of increased PI3Kγ, β2 adrenergic signaling could lead to a reduction in cardiac contractility. It would be interesting to determine the role PI3Kγ-regulated contractility in heart diseases. Moreover, inhibition of PI3Kγ may lead to better cardiac contractility in heart failure.

Experimental Procedures

Mutant Mice

The generation and genotyping of the PTEN-floxed, mckCRE, p110γ, and DN-p110α mice have been previously described (Suzuki et al., 2001; Bruning et al., 1998; Sasaki et al., 2000; Shioi et al., 2000; Hirsch et al., 2000). Only littermate mice were used as controls. Mice were bred and maintained following institutional guidelines.

Protein and mRNA Expression Analyses

Northern and Western blotting were carried out as described (Crackower et al., 2002) using antibodies to PTEN (Cascade), p110α, p110β, p110γ (Santa Cruz), p85 (Upstate Biotechnologies), phospho-AKT/PKB (S473), AKT/PKB, phospho-GSK3β, GSK3β, phospho-p70^{S6K}, phospho-ERK1/2, ERK1/2, phospho-phospholamban (Serine16), phospholamban (Cell Signaling Technology), and GAPDH (Research Diagnostics). For immunoprecipitations, lysates were incubated with anti-GRK2/3 Abs (Upstate Biotechnologies) conjugated with Sepharose beads for 16 hr at 4°C. Immunoprecipitates were separated using SDS–PAGE gel electrophoresis, transferred onto membranes, and immunoblotted.

Heart Morphometry, Echocardiography, and Hemodynamic Measurements

For heart morphometry, hearts were arrested with KCL, fixed with 10% buffered formalin, and embedded in paraffin. Fibrosis was analyzed using trichrome staining and quantitative morphometry using color-subtractive computer assisted image analysis. Echocardiographic assessments and invasive hemodynamic measurements were carried out as described (Crackower et al., 2002). Catecholamines were extracted from the plasma of male mice using alumina, eluted, and then assayed using HPLC (Waters Associates Inc., Milford, MA) coupled with electrochemical detection (ESA Inc., Bedford, MA). The intra-assay and inter-assay coefficient of variation were $<$5% and $<$10%, respectively.

Cardiomyocyte Purification

Adult ventricular myocytes were isolated as described (Sah et al., 2002). Cell size was measured using Openlab 2.2.5 software (Improvision Ltd). Ventricular myocytes were placed in a Plexiglas chamber and continuously perfused with oxygenated Tyrodes buffer (137 mM NaCl, 5.4 mM KCl, 10 mM glucose, 10 mM HEPES, 0.5 mM NaH_2PO_4, 1 mM $MgCl_2$, 1.2 mM $CaCl_2$, and [pH 7.4]) at 2.5 ml/min at 36°C. Neonatal ventricular cardiac myocytes were isolated from 1–3 day old mice in CBFHH buffer (137 mM NaCl, 5.36 mM KCl, 0.81 mM $MgSO_4 \cdot 7H_2O$, 5.55 mM dextrose, 0.44 mM KH_2PO_4, 0.34 mM $Na_2HPO_4 \cdot 7H_2O$, 20 μM Hepes, and [pH 7.4]) as described (Steinberg et al., 1991). Experiments were carried out 48–72 hr after plating.

Contractility Assays and cAMP Measurements

Cardiomyocytes were stimulated at 1 Hz with a Grass S44 stimulator (pulse duration 3 ms; 15–20 volts) and a video edge detector (Crescent Electronics) was used to track myocyte contractions at 240 Hz. Steady-state contractions were recorded at 1 kHz following a 4 min equilibrium period using a Phillips 800 camera system (240 Hz) and Felix acquisition software (Photon Technologies Inc.). Cardiomyocyte length, percent fractional shortening, shortening rate (+dL/dT), and relaxation rate (dL/dT) were determined at baseline. Myocytes were incubation with LY294002 (30 μM; Calbiochem) and Rp-cAMPS (25 μM; Sigma/RBI) for 10 min and recordings were made during continuous perfusion of the drug dissolved in Tyrode. In all experiments, phosphodiesterase activity was inhibited by pretreating the cells with theophylline (100 μM) for 30 min prior to stimulation. Wortmannin treatment (100 nM) was initiated at the time of theophylline addition. Zinterol (Bristol-Myers Squibb) stimulation was carried out at RT for 10 min. Forskolin (Sigma) was used at 25 μM. Isoproterenol (Sigma) stimulation was carried out at RT for 10 min, following 5 min pretreatment of ICI 118,551 (Sigma/RBI) (10^{-7}M). cAMP was measured by RIA according to the supplier's protocol (Amersham).

GRK Activity and β-Adrenergic Receptor Binding

GRK activity was measured by rhodopsin phosphorylation as described. Hearts were homogenized in 20 mM Tris [pH 7.3], 0.8 mM $MgCl_2$, and 2 mM EDTA. Membrane fractions were isolated by centrifuging at 40,000 *g* for 30 min at 4°C. Three hundred μg and twenty μg of protein were assayed for cytosolic and membrane fractions, respectively. β-AR density and affinity for its ligand ICYP (3-Iodocyanopindolol [^{125}I]) were determined by equilibrium radio-ligand binding assays on sarcolemmal membranes prepared from ventricular myocardium as described (Steinberg et al., 1995). Briefly, assays were performed with 30 μg membrane protein and ICYP (5-250 pM) in the absence or presence of 0.1 μM unlabeled propranolol to determine non-specific binding in a final volume of 1 ml for 60 min at 37°C. ICYP bound to membranes was separated from free, unbound ICYP by rapid vacuum filtration over glass-fiber filters (Gelman A/E).

Acknowledgments

We thank T. Wada, K Bachmaier, and S. Backman for helpful discussions. This study was supported by Amgen and by grants from American Heart Association and the NIH HL28958 to S.F.S. S.I. is supported by an NIH Grant, HL 65742. J.M.P. was supported by Amgen Inc., the National Cancer Institute of Canada, and IMBA, Vienna. J.M.P. holds a Canadian Research Chair in Cell Biology. M.A.C. is supported in part by a Canadian Institutes of Health Research fellowship.

Received: February 27, 2002
Revised: August 15, 2002

References

Alessi, D.R., Kozlowski, M.T., Weng, Q.P., Morrice, N., and Avruch, J. (1998). 3-Phosphoinositide-dependent protein kinase 1 (PDK1) phosphorylates and activates the p70 S6 kinase in vivo and in vitro. Curr. Biol. *8*, 69–81.

Backman, S.A., Stambolic, V., Suzuki, A., Haight, J., Elia, A., Pretorius, J., Tsao, M.S., Shannon, P., Bolon, B., Ivy, G.O., and Mak, T.W. (2001). Deletion of Pten in mouse brain causes seizures, ataxia and defects in soma size resembling Lhermitte-Duclos disease. Nat. Genet. *29*, 396–403.

Baliga, R.R., Pimental, D.R., Zhao, Y.Y., Simmons, W.W., Marchionni, M.A., Sawyer, D.B., and Kelly, R.A. (1999). NRG-1-induced cardiomyocyte hypertrophy. Role of PI-3-kinase, p70(S6K), and MEK-MAPK-RSK. Am. J. Physiol. *277*, H2026–H2037.

Bondeva, T., Pirola, L., Bulgarelli-Leva, G., Rubio, I., Wetzker, R., and Wymann, M.P. (1998). Bifurcation of lipid and protein kinase signals of PI3Kγ to the protein kinases PKB and MAPK. Science *282*, 293–296.

Brittsan, A.G., and Kranias, E.G. (2000). Phospholamban and cardiac contractile function. J. Mol. Cell. Cardiol. *32*, 2131–2139.

Bruning, J.C., Michael, M.D., Winnay, J.N., Hayashi, T., Horsch, D.,

Accili, D., Goodyear, L.J., and Kahn, C.R. (1998). A muscle-specific insulin receptor knockout exhibits features of the metabolic syndrome of NIDDM without altering glucose tolerance. Mol. Cell *2*, 559–569.

Colan, S.D. (1997). Mechanics of left ventricular systolic and diastolic function in physiologic hypertrophy of the athlete's heart. Cardiol. Clin. *15*, 355–372.

Crackower, M.A., Sarao, R., Oudit, G.Y., Yagil, C., Kozieradzki, I., Scanga, S.E., Oliveira-dos-Santos, A.J., da Costa, J., Zhang, L., Pei, Y., et al. (2002). Angiotensin-converting enzyme 2 is an essential regulator of heart function. Nature *417*, 822–828.

Di Cristofano, A., Pesce, B., Cordon-Cardo, C., and Pandolfi, P.P. (1998). Pten is essential for embryonic development and tumour suppression. Nat. Genet. *19*, 348–355.

Downward, J. (1998). Mechanisms and consequences of activation of protein kinase B/Akt. Curr. Opin. Cell Biol. *10*, 262–267.

Frank, K., and Kranias, E.G. (2000). Phospholamban and cardiac contractility. Ann. Med. *32*, 572–578.

Franke, T.F., Kaplan, D.R., Cantley, L.C., and Toker, A. (1997). Direct regulation of the Akt proto-oncogene product by phosphatidylinositol-3,4-bisphosphate. Science *275*, 665–668.

Hirsch, E., Katanaev, V.L., Garlanda, C., Azzolino, O., Pirola, L., Silengo, L., Sozzani, S., Mantovani, A., Altruda, F., and Wymann, M.P. (2000). Central role for G protein-coupled phosphoinositide 3-kinase γ in inflammation. Science *287*, 1049–1053.

Hunter, J.J., and Chien, K.R. (1999). Signaling pathways for cardiac hypertrophy and failure. N. Engl. J. Med. *341*, 1276–1283.

Kodama, H., Fukuda, K., Pan, J., Sano, M., Takahashi, T., Kato, T., Makino, S., Manabe, T., Murata, M., and Ogawa, S. (2000). Significance of ERK cascade compared with JAK/STAT and PI3-K pathway in gp130-mediated cardiac hypertrophy. Am. J. Physiol. Heart Circ. Physiol. *279*, H1635–H1644.

Komalavilas, P., Mehta, S., Wingard, C.J., Dransfield, D.T., Bhalla, J., Woodrum, J.E., Molinaro, J.R., and Brophy, C.M. (2001). PI3-kinase/Akt modulates vascular smooth muscle tone via cAMP signaling pathways. J. Appl. Physiol. *91*, 1819–1827.

Kuznetsov, V., Pak, E., Robinson, R.B., and Steinberg, S.F. (1995). β2-adrenergic receptor actions in neonatal and adult rat ventricular myocytes. Circ. Res. *76*, 40–52.

Leevers, S.J., Weinkove, D., MacDougall, L.K., Hafen, E., and Waterfield, M.D. (1996). The *Drosophila* phosphoinositide 3-kinase Dp110 promotes cell growth. EMBO J. *15*, 6584–6594.

Li, Z., Jiang, H., Xie, W., Zhang, Z., Smrcka, A.V., and Wu, D. (2000). Roles of PLC-β2 and -β3 and PI3Kγ in chemoattractant-mediated signal transduction. Science *287*, 1046–1049.

Lefkowitz, R.J. (1998). G protein-coupled receptors III. New roles for receptor kinanses and β-arrestins in receptor signalling and desensitization. J. Biol. Chem. *273*, 18677–18680.

Maehama, T., and Dixon, J.E. (1998). The tumor suppressor, PTEN/MMAC1, dephosphorylates the lipid second messenger, phosphatidylinositol 3,4,5-triphosphate. J. Biol. Chem. *273*, 13375–13378.

Matsui, T., Li, L., Wu, J.C., Cook, S.A., Nagoshi, T., Picard, M.H., Liao, R., and Rosenzweig, A. (2002). Phenotypic spectrum caused by transgenic overexpression of activated Akt in the heart. J. Biol. Chem. *277*, 22896–22901 Published online April 9, 2002. 10.1074/jbc.M200347200.

Milligan, G., and White, J.H. (2001). Protein-protein interactions at G-protein-coupled receptors. Trends Pharmacol. Sci. *22*, 513–518.

Minamisawa, S., Hoshijima, M., Chu, G., Ward, C.A., Frank, K., Gu, Y., Martone, M.E., Wang, Y., Ross, J., Jr., Kranias, E.G., et al. (1999). Chronic phospholamban-sarcoplasmic reticulum calcium ATPase interaction is the critical calcium cycling defect in dilated cardiomyopathy. Cell *99*, 313–322.

Naga Prasad, S.V., Esposito, G., Mao, L., Koch, W.J., and Rockman, H.A. (2000). G$\beta\gamma$-dependent phosphoinositide 3-kinase activation in hearts with in vivo pressure overload hypertrophy. J. Biol. Chem. *275*, 4693–4698.

Naga Prasad, S.V., Barak, L.S., Rapacciuolo, A., Caron, M.G., and Rockman, H.A. (2001a). Agonist-dependent recruitment of phosphoinositide 3-kinase to the membrane by β-adrenergic receptor kinase 1. A role in receptor sequestration. J. Biol. Chem. *276*, 18953–18959.

Naga Prasad, S.V., Nienaber, J., and Rockman, H.A. (2001b). β-adrenergic axis and heart disease. Trends Genet. *17*, S44–S49.

Rabkin, S.W., Goutsouliak, V., and Kong, J.Y. (1997). Angiotensin II induces activation of phosphatidylinositol 3-kinase in cardiomyocytes. J. Hypertens. *15*, 891–899.

Rockman, H.A., Koch, W.J., and Lefkowitz, R.J. (2002). Seven-transmembrane-spanning receptors and heart function. Nature *415*, 206–212.

Sah, R., Oudit, G.Y., Nguyen, T.T., Lim, H.W., Wickenden, A.D., Wilson, G.J., Molkentin, J.D., and Backx, P.H. (2002). Inhibition of calcineurin and sarcolemmal Ca2+ influx protects cardiac morphology and ventricular function in K(v)4.2N transgenic mice. Circulation *105*, 1850–1856.

Sasaki, T., Irie-Sasaki, J., Jones, R.G., Oliveira-dos-Santos, A.J., Stanford, W.L., Bolon, B., Wakeham, A., Itie, A., Bouchard, D., Kozieradzki, I., et al. (2000). Function of PI3Kγ in thymocyte development, T cell activation, and neutrophil migration. Science *287*, 1040–1046.

Scanga, S.E., Ruel, L., Binari, R.C., Snow, B., Stambolic, V., Bouchard, D., Peters, M., Calvieri, B., Mak, T.W., Woodgett, J.R., and Manoukian, A.S. (2000). The conserved PI3′K/PTEN/Akt signaling pathway regulates both cell size and survival in *Drosophila*. Oncogene *19*, 3971–3977.

Schluter, K.D., Simm, A., Schafer, M., Taimor, G., and Piper, H.M. (1999). Early response kinase and PI 3-kinase activation in adult cardiomyocytes and their role in hypertrophy. Am. J. Physiol. *276*, H1655–H1663.

Schwartzbauer, G., and Robbins, J. (2001). The tumor suppressor gene PTEN can regulate cardiac hypertrophy and survival. J. Biol. Chem. *276*, 35786–35793.

Shima, H., Pende, M., Chen, Y., Fumagalli, S., Thomas, G., and Kozma, S.C. (1998). Disruption of the p70(s6k)/p85(s6k) gene reveals a small mouse phenotype and a new functional S6 kinase. EMBO J. *17*, 6649–6659.

Shioi, T., Kang, P.M., Douglas, P.S., Hampe, J., Yballe, C.M., Lawitts, J., Cantley, L.C., and Izumo, S. (2000). The conserved phosphoinositide 3-kinase pathway determines heart size in mice. EMBO J. *19*, 2537–2548.

Shioi, T., McMullen, J.R., Kang, P.M., Douglas, P.S., Obata, T., Franke, T.F., Cantley, L.C., and Izumo, S. (2002). Akt/protein kinase B promotes organ growth in transgenic mice. Mol. Cell. Biol. *22*, 2799–2809.

Steinberg, S.F., Robinson, R.B., Lieberman, H.B., Stern, D.M., and Rosen, M.R. (1991). Thrombin modulates phosphoinositide metabolism, cytosolic calcium, and impulse initiation in the heart. Circ. Res. *68*, 1216–1229.

Steinberg, S.F., Zhang, H., Pak, E., Pagnotta, G., and Boyden, P.A. (1995). Characteristics of the β-adrenergic receptor complex in the epicardial border zone of the 5-day infarcted canine heart. Circulation *9*, 2824–2833.

Stephens, L., Eguinoa, A., Corey, S., Jackson, T., and Hawkins, P.T. (1993). Receptor stimulated accumulation of phosphatidylinositol (3,4,5)-trisphosphate by G-protein mediated pathways in human myeloid derived cells. EMBO J. *12*, 2265–2273.

Suzuki, A., de la Pompa, J.L., Stambolic, V., Elia, A.J., Sasaki, T., del Barco Barrantes, I., Ho, A., Wakeham, A., Itie, A., Khoo, W., et al. (1998). High cancer susceptibility and embryonic lethality associated with mutation of the PTEN tumor suppressor gene in mice. Curr. Biol. *8*, 1169–1178.

Suzuki, A., Yamaguchi, M.T., Ohteki, T., Sasaki, T., Kaisho, T., Kimura, Y., Yoshida, R., Wakeham, A., Higuchi, T., Fukumoto, M., et al. (2001). T cell-specific loss of Pten leads to defects in central and peripheral tolerance. Immunity *14*, 523–534.

Tamura, M., Gu, J., Matsumoto, K., Aota, S., Parsons, R., and Yamada, K.M. (1998). Inhibition of cell migration, spreading, and focal adhesions by tumor suppressor PTEN. Science *280*, 1614–1617.

Toker, A., and Cantley, L.C. (1997). Signalling through the lipid products of phosphoinositide-3-OH kinase. Nature *387*, 673–676.

Yusuf, S., Reddy, S., Ounpuu, S., and Anand, S. (2001). Global burden of cardiovascular diseases Part I: General considerations, the epidemiologic transition, risk factors, and impact of urbanization. Circulation *104*, 2746–2753.

Xiao, R.P., Avdonin, P., Zhou, Y.Y., Cheng, H., Akhter, S.A., Eschenhagen, T., Lefkowitz, R.J., Koch, W.J., and Lakatta, E.G. (1999). Coupling of β2-adrenoceptor to Gi proteins and its physiological relevance in murine cardiac myocytes. Circ. Res. *84*, 43–52.

Zvaritch, E., Backx, P.H., Jirik, F., Kimura, Y., de Leon, S., Schmidt, A.G., Hoit, B.D., Lester, J.W., Kranias, E.G., and MacLennan, D.H. (2000). The transgenic expression of highly inhibitory monomeric forms of phospholamban in mouse heart impairs cardiac contractility. J. Biol. Chem. *275*, 14985–14991.